Hydrothermal synthesis and characterization of novel aloe-like SnS_2 nanostructures

HONGLIANG ZHU*
Center of Materials Engineering, Zhejiang Sci-Tech University, Xiasha University Town, Hangzhou 310018, People's Republic of China; State Key Lab of Silicon Materials, Zhejiang University, Hangzhou 310027, People's Republic of China
E-mail: webmaster@51yq.com

XIN JI
College Of Chemistry and Chemical Engineering, Henan University, Kaifeng 475001, People's Republic of China

DEREN YANG
State Key Lab of Silicon Materials, Zhejiang University, Hangzhou 310027, People's Republic of China

Published online: 12 April 2006

Novel aloe-like tin bisulfide (SnS_2) nanostructures were successfully synthesized via a thioglycolic acid (TGA) assisted hydrothermal process. X-ray powder diffraction (XRD), transmission electron microscopy (TEM) and field emission scanning electron microscopy (FESEM) were used to characterize the product. XRD pattern reveals that the product is well-crystallized SnS_2 with hexagonal structure. TEM and FESEM images clearly show an aloe-like nanostructure that is made from several single crystalline leaves. Furthermore, the possible growth mechanism is discussed.
© *2006 Springer Science + Business Media, Inc.*

1. Introduction

Nowadays, one of the important goals of material scientists is to develop ways of tailoring the structure of materials to obtain specific nanomorphologies [1, 2]. Interesting nanomorphologies and specific structures have been sparking much attention because of their remarkable electrical, optical and magnetic properties [3]. Inorganic materials with different morphologies can exhibit different properties, even if they are made up of the same elements. Therefore, synthesis of nanostructures of novel morphologies is especially attractive for nanoscience and nanotechnology. Herein, we report hydrothermal synthesis and characterization of novel aloe-like SnS_2 nanostructures.

SnS_2 has attracted much attention for its semiconducting and optical properties. SnS_2, a lamellar structure semiconductor with a band gap of around 2.35 eV [4], can be potentially used as an efficient solar cell material [5]. It is also of interest in holographic recording systems and electrical switching [6, 7]. Additionally, SnS_2 can be used as an optical material because it exhibits a strong anisotropy of optical properties [8].

Tin sulfides show a variety of phases, such as SnS, Sn_2S_3, Sn_3S_4 and SnS_2, due to the versatile coordinating characteristics of tin and sulfur [9]. Of these compounds, SnS and SnS_2 are more attractive for their interesting properties. Conventionally, tin sulfides have been prepared by chemical vapour deposition (CVD) [10, 11], by electrochemical deposition [12], by molecular beam epitaxy (MBE) [13], and by spray pyrolysis [14]. In recent years, a number of synthesis processes have been employed to prepare SnS_2 nanocrystallines, including solvothermal method [15, 16], hydrothermal synthesis [17, 18], microwave-assisted polyol synthetic method [19], laser ablation [20] and template-assisted solvent-relief process [21]. Our group has reported the preparation of single-crystalline SnS_2 nano-belts by a thioglycolic (TGA, $C_2H_4O_2S$) assisted hydrothermal method [22]. More interestingly, various SnS_x nanostructures have been prepared via the TGA-assisted hydrothermal synthesis by

*Author to whom all correspondence should be addressed.
0022-2461 © *2006 Springer Science + Business Media, Inc.*
DOI: 10.1007/s10853-005-5911-y

changing the hydrothermal temperature and the mol ratio of the reactants. It is reasonable to believe that the TGA-assisted hydrothermal process offers great opportunities for the preparation of tin chalcogenide nanostructures.

2. Experimental

All reagents were of analytical grade without further purification. 0.001 mol of $SnCl_2{\cdot}2H_2O$ powder and 50 μL of thioglyeolic acid (TGA) were added to 100 ml of Na_2S solution with a concentration of 0.04 M under stirring, meaning that the mol ratio of Sn^{2+}:S^{2-} was 1:4. After 10 min stirring, the final aqueous solution was transferred into a Teflon-lined autoclave of 120 ml capacity. The autoclave was maintained at 160°C for 24 h, and then cooled to room temperature naturally. The product was centrifuged and rinsed with alcohol and deionized water for 3 times, finally dried at 60°C for 30 min in air.

X-ray diffraction (XRD) pattern was obtained on a Rigaku D/max-ga X-ray diffractometer with graphite monochromatized CuKa radiation ($\lambda = 1.54178$ Å). Transmission electron microscopy (TEM) observation was performed on a Philips CM200 high-resolution transmission electron microscope (HRTEM) with an accelerating voltage of 200 kV. Scanning electron microscopy (SEM) observation was performed on a FEI SIRION field-emission scanning electron microscope (FESEM).

3. Results and discussion

The XRD pattern of the as-prepared sample is shown in Fig. 1. All the diffraction peaks can be indexed to hexagonal SnS_2 with lattice constants $a = 3.648$, $c = 5.899$ Å, which is in good agreement with the values in the standard card (JCPDS No. 23-0677). No impurity peaks such as those of SnO_2, SnS or SnO were detected. The strong and sharp peaks indicate that the SnS_2 product is well crystallized. Average crystalline size has been estimated by the Scherrer's formula:

$$D = K \cdot \lambda/(\beta \cdot \cos\theta), \tag{1}$$

where $K = 0.9$ is the shape factor, λ is the X-ray wavelength of Cu Kα radiation (0.154 nm), θ is the Bragg angle, and β is the experimental full-width half maxium (FWHM) of the respective diffraction peak (in units of radians). Consequently, the grain size of the product was estimated to be around 40 nm.

Typical TEM and FESEM images are shown in Fig. 2. Fig. 2a reveals that each SnS_2 nanostructure is composed of several nano-leaves approximately 50 nm in width and 200 nm in length. Interestingly, these nano-leaves circle around a center, demonstrating a radially symmetric structure; two adjacent nano-leaves form a 60-degree angle, meaning that the SnS_2 nanostructures exhibit obvious six-fold symmetry due to hexagonal structure of SnS_2. Therefore, it can be concluded that the nanostructures have six symmetric preferential growth directions. Fig. 2b and c

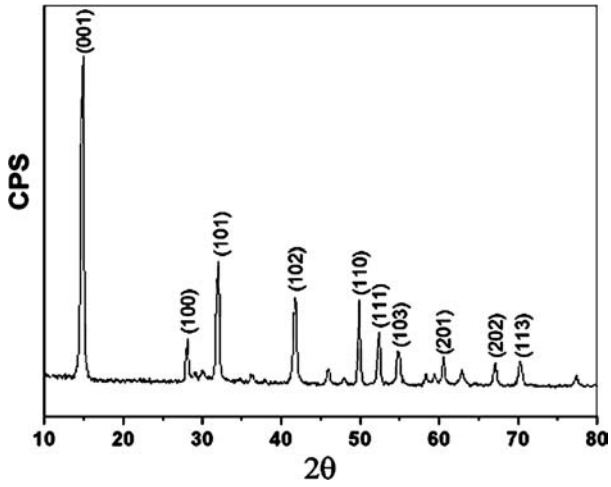

Figure 1 XRD pattern of the aloe-like SnS_2 nanostructures.

clearly show that several nano-leaves are self-assembled into an "aloe". The definition of the aloe-like SnS_2 nanostructures comes from the geometrical similarity to aloes. Additionally, the FESEM images reveal that there are several nano-leaves along central axis of the aloe-like nanostructures besides the radially symmetric nano-leaves. We attribute the formation of the nano-leaves along central axis to preferential growth along [0001] direction.

The energy dispersive X-ray (EDX) spectrum of the SnS_2 nanostructures is shown in Fig. 3. The strong peaks of Sn and S are found in the spectrum. The C and Cu peaks come from the carbon-coated copper grid used to support the sample. Additional structure characterization was carried out using high-resolution transmission electronic microscopy (HRTEM), and the typical HRTEM image of one of radially symmetric nano-leaves is shown in Fig. 4. Fig. 4 clearly shows the fringes with a lattice spacing of about 0.316 nm, which correspond to $\{100\}$ planes of hexagonal SnS_2 (JCPDS No. 23-0677). Furthermore, Fig. 4 identifies that the nano-leaf is structurally uniform single crystalline in nature. More interestingly, as shown in Fig. 4, $\{100\}$ planes are perpendicular to the length axis of the nano-leaf, the preferential growth direction of the nano-leaf. The HRTEM images of other nanoleaves were similar to that of Fig. 4. In addition to six-fold radial symmetry of the radially growing nano-leaves and aloe-like morphology of the nanostructures, we conclude that the formation of the radially growing nano-leaves was due to preferential growth along $\langle 10\bar{1}1\rangle$directions.

Previously, thioglyeolic acid (TGA) was widely used as a stability agent preventing nano-crystals from aggregating [23, 24]. In our synthetic route, TGA is critical for the formation of the aloe-like SnS_2 nanostructures. The detailed chemical mechanism can be expressed as follows:

$$SnCl_2 + H_2O \Leftrightarrow Sn(OH)Cl \downarrow + HCl \tag{2}$$

$$Sn(OH)Cl \downarrow + Na_2S \Leftrightarrow SnS \downarrow + NaCl + NaOH \tag{3}$$

$$SnS \Leftrightarrow Sn^{2+} + S^{2-} \tag{4}$$

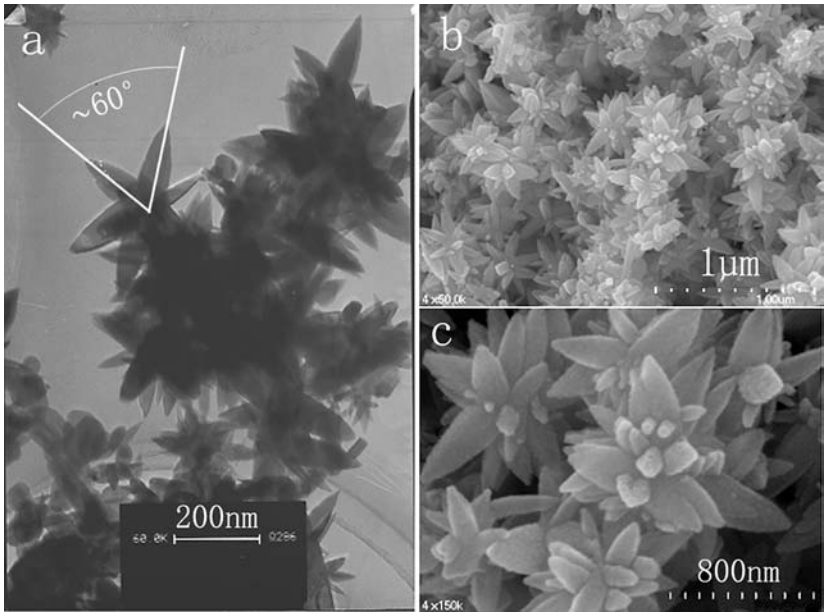

Figure 2 TEM and FESEM images of the aloe-like SnS_2 nanostructures: (a) TEM image; (b) FESEM image; (c) amplified FESEM image.

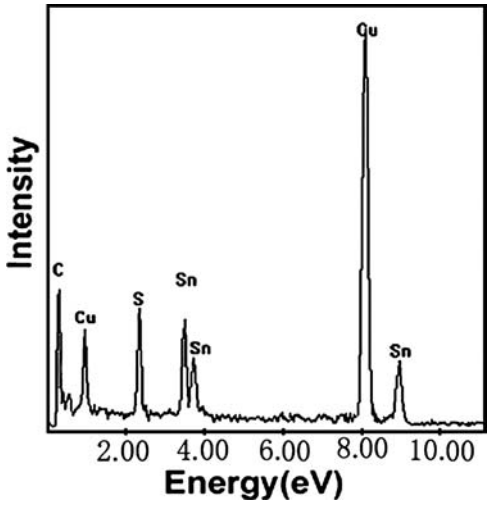

Figure 3 EDX spectrum of the aloe-like SnS_2 nanostructures.

$$Sn^{2+} + 2H^+ + O_2 \Leftrightarrow Sn^{4+} + 2H_2O \quad (5)$$

$$Sn^{4+} + 2S^{2-} \Leftrightarrow SnS_2 \downarrow \quad (6)$$

$$mSnS_2 + kHSCH_2COOH + kSn^{4+} \Leftrightarrow (SnS_2)_m(SnSCH_2COOH)_k^{3k+} + kH^+ \quad (7)$$

$$(SnS_2)_m(SnSCH_2COOH)_k^{3k+} \rightarrow (SnS_2)_m(Sn^{4+})_k + kSCH_2COOH^- \quad (8)$$

$$(SnS_2)_m(Sn^{4+})_k + 2kS^{2-} \rightarrow (m+k)SnS_2 \quad (9)$$

Prior to the hydrothermal process, the hydrolysis of $SnCl_2$ and the formation of SnS nuclei were carried out via reactions (2) and (3), respectively. Due to the excess of S^{2-}, SnS_2 nuclei were formed in the hydrothermal process according to reactions (4)–(6). Compared with the conventional hydrothermal process, in the TGA-assisted hydrothermal process the marked difference is the formation of $(SnS_2)_m(SnSCH_2COOH)_k^{3k+}$ complex clusters in the solution via reaction (7). Reaction (8) represents the dissociation of SCH_2COOH^- from the SnS_2 complex clusters. Furthermore, we believe that the dissociation of SCH_2COOH^- occurs in a local region of the

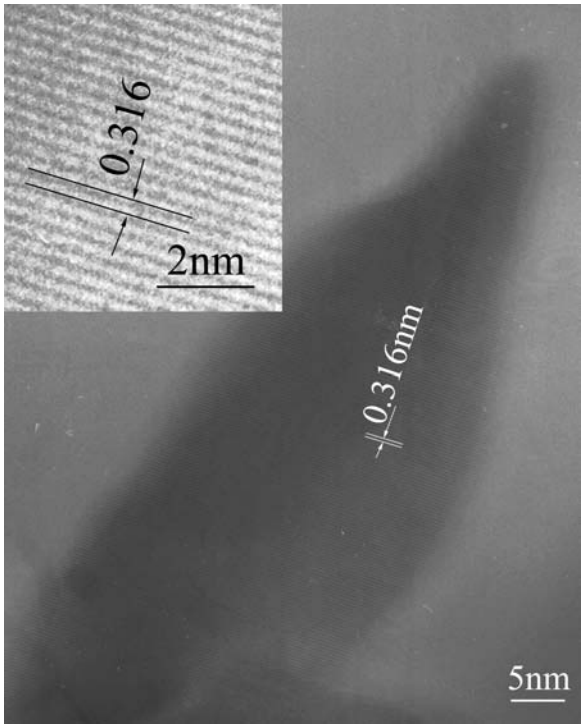

Figure 4 HRTEM image of a single nano-leaf of the SnS_2 nanostructures.

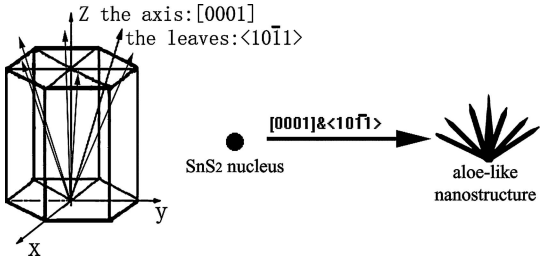

Figure 5 A sketch of growth mechanism of the aloe-like SnS_2 nanostructures.

complexed SnS_2 cluster, where there are Sn^{4+} exposed to the S^{2-} existing in the solution. Therefore, during the TGA-assisted hydrothermal process, the formation of SnS_2 proceeds along specific directions. Following the basic idea of the hydrothermal process introduced in this paper, we have successfully prepared SnS_2 nano-belts [22], Bi_2S_3 nanowires [25], CdS nanorods [26] and PbS start-shaped crystals [27] by the TGA-assisted hydrothermal method.

The formation of the novel aloe-like nanostructures is an interesting subject. Jinwoo Cheon *et al*. reported that the final shape of the obtained crystals is determined by competitive growth on different crystalline faces [28]. According to above discussion, there are two kinds of nano-leaves: the radially symmetric nano-leaves and the nano-leaves along central axis of the aloe-like nanostructures. Furthermore, it has been concluded that the formation of these two kinds of nano-leaves is due to preferential growth along $\langle 10\bar{1}1\rangle$directions and [0001] direction, respectively. Therefore, a sketch of possible growth mechanism was put forward and shown in Fig. 5. The two kinds of preferential growth directions, namely,$\langle 10\bar{1}1\rangle$ directions and [0001] direction, are illustrated in Fig. 5. Frankly, the above explanation is somewhat conjectural and phenomenological.

4. Conclusion

In summary, novel aloe-like tin bisulfide (SnS_2) nanostructures have been successfully prepared by a thioglycolic acid (TGA) assisted hydrothermal method. XRD pattern reveals that the product is well-crystallized SnS_2 with hexagonal structure. TEM and FESEM images clearly show an aloe-like nanostructure that is made from several single crystalline nano-leaves. Based on FESEM, TEM and HRTEM images of the SnS_2 product with hexagonal structure, possible growth mechanism has been discussed. Furthermore, it is reasonable to believe that the TGA-assisted hydrothermal process offers great opportunities for preparation of tin chalcogenide nanostructures.

Acknowledgment

The authors would like to appreciate the financial supports of 863 project (No. 2001AA513023), the Natural Science Foundation of China (No. 60225010) and the Zhejiang Provincial Natural Science Foundation of China (No. 601092). We also thank Prof. Youwen Wang for the SEM measurements.

References

1. S. LIJIMA, *Nature (London)* **354** (1991) 56.
2. N.G. CHOPRA, R.J. LUYKEN, K. CHERREY, V.H. CRESPI, M.L. COHEN, S.G. LOUIE and A. ZETTL, *Science* **269** (1995) 966.
3. A.M. RAO, E. RICHTER, S. BANDOW, B. CHASE, P.C. EKLUND, K.A. WILLIAMS, S. FANG, K.R. SUBBASWAMY, M. MENON, A. THESS, R.E. SMALLEY, G. DRESSELHAUS and M.S. DRESSELHAUS, *Science* **275** (1997) 187.
4. C.D. LOKHANDE, *J. Phys. D: Appl. Phys.* **23** (1990) 703.
5. J.J. LOFERSKI, *J. Appl. Phys.* **27** (1956) 777.
6. D. CHU, R.M. WALSER, R.W. BENE and T.H. COURTNEY, *Appl. Phys. Lett.* **24** (1974) 479.
7. S.G. PATIL and R.H. FREDGOLD, *J. Pure Appl. Phys.* **4** (1971) 718.
8. A. AGARWAL, P.D. PATEL and D. LAKSHMINARAYANA, *J. Cryst. Growth* **142** (1994) 344.
9. T. JIANG and G.A. OZIN, *J. Mater. Chem.* **8** (1998) 1099.
10. L.S. PRICE, I. P. PARKIN, T.G. HIBBERT and K.C. MOLLOY, *Chem. Vapor Depos.* **4** (1998) 222.
11. T. SHIBATA, T. MIURA, T. KISHI and T. NAGAI, *J. Cryst. Growth* **106** (1990) 593.
12. A. GHAZALI, Z. ZAINAL, M.Z. HUSSEIN and A. KASSIM, *Sol. Energy Mater. Sol. Cells* **55** (1998) 237.
13. K.W. NNEBESNY, G.E. COLLINS, P.A. LEE, L.K. CHAU, J. DANZIGER, E. OSBURN and N.R. ARMSTRONG, *Chem. Mater.* **3** (1991) 829.
14. A. ORTIZ and S. LOPEZ, *Semicond. Sci. Technol.* **9** (1994) 2130.
15. Q. LI, Y. DING, H. WU, X. LIU and Y. QIAN, *Mate. Res. Bull.* **37** (2002) 925.
16. B. HAI, K. TANG, C. WANG, C. AN, Q. YANG, G. SHEN and Y. QIAN, *J. Cryst. Growth* **225** (2001) 92.
17. X. GOU, J. CHEN and P. SHEN, *Mater. Chem. Phys.* **93** (2005) 557.
18. C. WANG, K. TANG, Q. YANG, Y. QIAN and C. XU, *Chem. Lett.* (2001) 1294.
19. D. CHEN, G. SHEN, K. TANG, S. LEI, H. ZHENG and Y. QIAN, *J. Cryst. Growth* **260** (2004) 469.
20. S. HONG, R. POPOVITZ-BIRO, Y. PRIOR and R.J. TENNE, *J. Am. Chem. Soc.* **125** (2003) 10470.
21. D. CHEN, G. SHEN, K. TANG, Y. LIU and Y. QIAN, *Appl. Phys. A-Mater.* **77** (2003) 747.
22. Y. JI, H. ZHANG, X. MA, J. XU and D. YANG, *J. Phys.: Condens. Matter* **15** (2003) L661.
23. M. GAO, S. KIRSTEIN and H. MOHWALD, *J. Phy. Chem. B* **102** (1998) 8360.
24. D. HAYS, O. MIEIE, M. NENADOVIE, V. SWAYAMBUNATHAN and D. MEISEL, *J. Phys. Chem.* **93** (1989) 4603.
25. H. ZHANG, Y. JI, X. MA, J. XU and D. YANG, *Nanotechnology* **14** (2003) 974.
26. H. ZHANG, X. MA, Y. JI, J. XU and D. YANG, *Chem. Phys. Lett.* **377** (2003) 654.
27. Y. JI, X. MA, H. ZHANG, J. XU and D. YANG, *J. Phys.: Condens. Matter* **15** (2003) 7611.
28. S.M. LEE, S.N. CHO and J.W. CHEON, *Adv. Mater.* **15** (2003) 441.

Received 17 February
and accepted 29 July 2005